Original Research Article

Numerical Study on Micropolar Nanofluid Flow over an Inclined Surface by Means of Keller-Box

Abstract

In this paper, micropolar nanofluid boundary layer flow over a linear inclined stretching surface with the magnetic effect is investigated. Buongiorno's model utilized in this study for the thermal efficiencies of the fluid flow in the presence of Brownian motion and thermophoresis properties. The nonlinear problem for micropolar nanofluid flow over an inclined sheet is established to study the heat and mass exchange phenomenon by considering portent flow parameters to strengthen the boundary layers. The governing nonlinear partial differential equations are changed to nonlinear ordinary differential equations by using suitable similarity transformations and then solved numerically by applying the Keller-Box method. A comparison of the setup results in the absence of the incorporated impacts is performed with the accessible results and perceived in a decent settlement. Numerical and graphical outcomes are additionally presented in tables and diagrams.

Keywords: Micropolar nanofluid, MHD, inclined surface.

1 Introduction

Nanofluids set up a subclass of molecular liquids designed to work at the nanoscale. Nanofluids constitute relation between bulk materials and molecular structure. The fast development of nanotechnology has witnessed a noteworthy attention in such liquids through the whole breadth of manufacturing, including engineering, aerospace, medical productions and energy technologies. Nanofluid is a mixure of various nanoparticles, for example, aluminum, silver, copper and titanium with or without their oxides and base liquids including water, ethylene glycol and oil and so on. when nanoparticles strategically dispersed in the base fluids, the resulting nanofluids have been confirmed to attain a significant improvement in the properties of thermal conductivity, presented by Choi [1]. The elements that play essential principle to upgrade the thermal conductivity of nanofluid have been considered by Buongiorno [2]. He found that the thermal conductivity of the fluid increment due to thermophoresis and Brownian movement impacts in the ordinary liquid. Brownian movement is the unpredictable development of the nanoparticles in the conventional liquid and caused the constant impacts between based liquid and nanoparticles. Thermophoresis is the wonder which diffuses the particles because of

the temperature inclination. The heat transfer of nanofluid over a nonlinear porous sheet is numerically discussed by Zaimi et al. [3]. Anwar et al. [4] considered the numerical investigation of micropolar nanofluid flow over an extending sheet. Nanofluid flow over a slanted extending surface was studied by Sandeep and Kumar [5]. Suriyakumar and Devi [6] discussed the impacts of internal heat generation and suction on mixed convective nanofluid flow through a slanted surface. Ziaei-Rad et al. [7] examined the similarity solution of boundary layer nanofluid flow on an inclined surface[37]. Rashad [8] studied nanofluid flow by considering convective boundaries and anisotropic slip effect. Mitra [9] investigated computational modeling of nanofluid flow over a heated inclined plate. Khan et al. [10] outlined the heat and mass exchange of MHD Jeffery nanofluid flow over slanted sheet. Hatami et al. [11] examined three dimensional relentless nanofluid over a slanted plate. For latest literature on nanofluid flow over an inclined sheet, see [12-14].

The boundary layer flow over an inclined extending surface turn into an intriguing field of research on account of its uses in building, for example, paper creation, skin rubbing, grain stockpiling and drag generation. The investigation of boundary layer flow over constant surface was begun by Sakiadis [15]. Also, Crane [16] examined the closed form arrangement of boundary layer flow over an extending sheet. The boundary layer flow of dusty liquid over a slanted surface with heat source/sink was introduced by Ramesh et al. [17]. Singh [18] explored heat and mass exchange of thick liquid on porous slanted plate. Similarity solution of magnetohydrodynmaic flow over a slanted sheet was examined by Ali et al. [19]. Ramesh et al. [20] took a shot at the boundary layer flow over slanted sheet with convective limits. MHD free convection dissipative liquid flow past over a slanted permeable surface was examined by Malik [21]. Hayat et al. [22] investigated radiation effect on the flow induced by stretching cylinder by considering non-uniform heat source/sink. Balla et al. [23] examined an inclined porous cavity filled with nanofluid saturated in permeable medium. The boundary layer flow over an inclined sheet with different impacts, see [24-25].

Micropolar liquids are those, which contain rigid arbitrarily oriented particles immersed in a sticky medium with microstructure constituent, where bending of the molecule is unnoticed. Eringen [26] built up another philosophy of micropolar liquid to check the impact of small scale revolutions on fluid movement. Rahman et al. [27] talked about the flow of micropolar fluid by thinking about the variable properties. Micropolar fluid flow by taking different effects over an inclined sheet was studied by Das [28]. Kasim et al. [29] inspected the micropolar fluid flow on the slanted plate numerically. Srinivasacharya and Bindu [30] researched micropolar fluid move through a slanted channel having parallel plates. Hazbavi and Sharhani [31] analyzed the flow of micropolar fluid between two parallel plates with steady weight slope. Shamshuddin et al. [32] contemplated the heat and mass exchange of micropolar liquid flow through penetrable slanted plate. The impact of two fold scattering on micropolar liquid flow over a slanted surface was examined by Srinivasacharya et al. [33].

2 Problem formulation

A steady, two dimensional boundary layer flow of micropolar nanofluid over a permeable inclined linear stretching plate with an angle γ is considered. The stretching and free stream velocities are supposed to be as, $u_w(x) = ax$ and $u_\infty(x) = 0$ respectively, here 'x' is the coordinate dignified lengthways the enlarging surface and 'a' is a constant. An external transverse magnetic field is taken normal to the flow path. It is supposed that the electric and magnetic field effects are very minor as the magnetic Reynolds number is less, Mishra et al. [34].The micropolar finite size particles along with Nano particles are constantly distributed in the base fluids. The fluid particles have extra space to travel about formerly hitting to the other fluid particle, where these particles revolve in the fluid field and fallouts for spinning effects in the micropolar nanofluid. The Brownian motion and thermophoresis effects are taken into account. The temperature T and nano particle fraction C at the wall take the constant values T_w and C_w, while the ambient forms used for nanofluid temperature and mass fractions T_∞ and C_∞ are attained as *y* lean towards to immensity shown in fig.1.

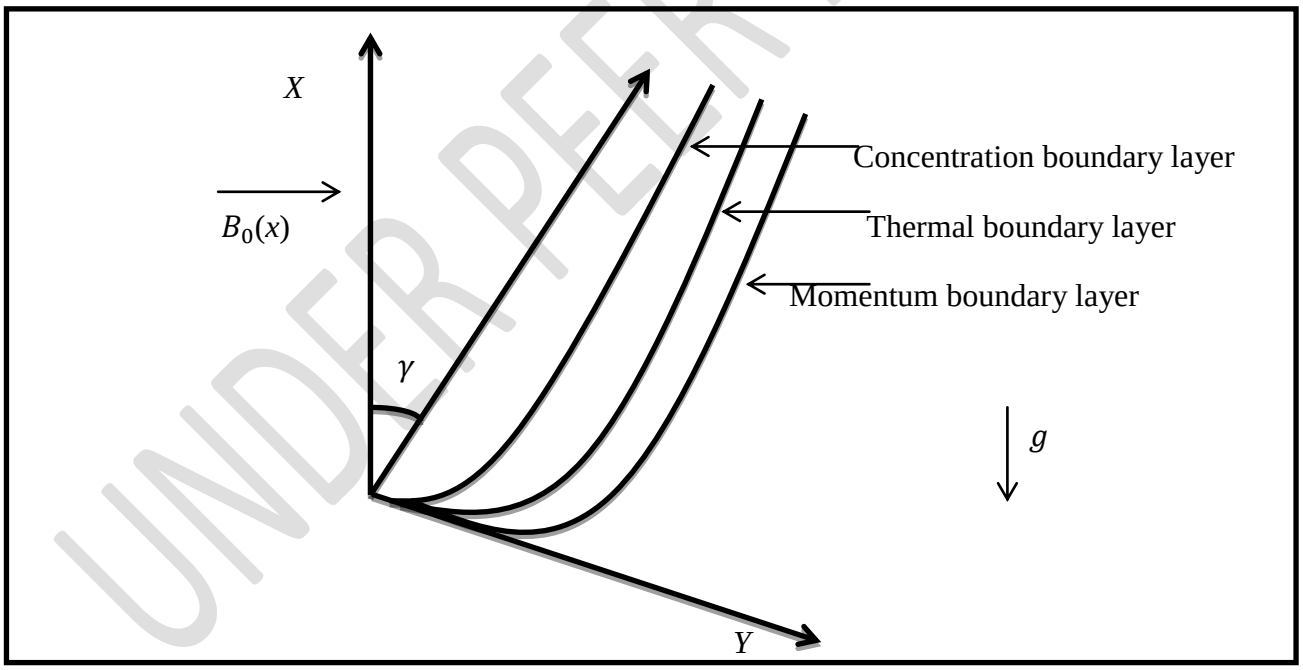

Fig.1. Physical geometry and coordinate system

The flow equations for this study are given by

$$\frac{\partial u}{\partial x}+\frac{\partial v}{\partial y}=0, \tag{1}$$

$$u\frac{\partial u}{\partial x}+v\frac{\partial u}{\partial y}=\left(\frac{\mu+K_1^*}{\delta}\right)\frac{\partial^2 u}{\partial y^2}+\left(\frac{K_1^*}{\rho}\right)\frac{\partial N^*}{\partial y}+g[\beta_t(T-T_\infty)-\beta_c(C-C_\infty)]cos\gamma-(\frac{\sigma {B_0}^2(x)}{\rho}+\frac{\mu}{\rho k})u, \tag{2}$$

$$u\frac{\partial N^*}{\partial x}+v\frac{\partial N^*}{\partial y}=\left(\frac{\gamma^*}{j^*\delta}\right)\frac{\partial^2 N^*}{\partial y^2}-\left(\frac{{K_1}^*}{j^*\delta}\right)\left(2N^*+\frac{\partial u}{\partial y}\right), \tag{3}$$

$$u\frac{\partial T}{\partial x}+v\frac{\partial T}{\partial y}=\alpha\frac{\partial^2 T}{\partial y^2}+\tau\left[D_B\frac{\partial C}{\partial y}\frac{\partial T}{\partial y}+\frac{D_T}{T_\infty}\left(\frac{\partial T}{\partial y}\right)^2\right], \tag{4}$$

$$u\frac{\partial C}{\partial x}+v\frac{\partial C}{\partial y}=D_B\frac{\partial^2 C}{\partial y^2}+\frac{D_T}{T_\infty}\frac{\partial^2 T}{\partial y^2}, \tag{5}$$

Where in the directions x and y the velocity constituents are u and v, individually, g is the gravitational acceleration, the uniform magnetic field strength is given by B_0, σ denotes the electrical conductivity, the viscosity is denoted by μ, the density of the base liquid is given by δ_f, the density of the nanoparticle is given by δ_p, the vortex viscosity is defined as k_1^*, factor of thermal increase is given by β_t, β_c denotes constant of concentration extension, the gyration ascent viscosity is given by γ^*, j^* is the micro inertia per unit mass, the micro-rotation is given by N^*, D_B denote the Brownian dispersal factor and D_T denotes the thermophoresis dispersion amount, k is the thermal conductivity, the heat capacity of the nanoparticles is denoted by $(\delta c)_p$, $(\delta c)_f$ represents the heat capacity of the conventional liquid, thermal diffusivity parameter is denoted by $\alpha=\frac{k}{(\delta c)_f}$ and the relation among the active heat capacity of the nanoparticle and heat capacity of the liquid is represented by $\tau=\frac{(\delta c)_p}{(\delta c)_f}$.

The subject boundary conditions are

$$u=u_w(x)=ax, v=0, T=T_w, N^*=-m_0\frac{\partial u}{\partial y}, C=C_w \quad at \quad y=0,$$

$$u\to u_\infty(x)=0, v\to 0, T\to T_\infty, N^*\to 0, \quad C\to C_\infty \quad at \quad y\to\infty, \tag{6}$$

The nonlinear ordinary differential equations are obtained from nonlinear partial differential equations. The stream function $\psi=\psi(x,y)$ use for this procedure is given as

$$u=\frac{\partial\psi}{\partial y}, \quad v=-\frac{\partial\psi}{\partial x}, \tag{7}$$

Where, equation (1) i.e. continuity equation is fulfilled identically. The similarity transformations are characterized as

$$u = axf'(\eta), v = -\sqrt{av}f(\eta), \eta = y\sqrt{\frac{a}{v}}$$

$$\theta(\eta) = \frac{T-T_\infty}{T_w-T_\infty}, \phi(\eta) = \frac{C-C_\infty}{C_w-C_\infty}, \quad (8)$$

On substituting equation (8), system of equations (2) to (5) are converted to the following nonlinear ordinary differential equations:

$$(1+k)f''' + ff'' - f'^2 + kh' + (\lambda g + \delta q)cos\gamma - (M+K_1)f' = 0, \quad (9)$$

$$\left(1+\frac{k}{2}\right)h'' + fh' - f'h - k(2h+f'') = 0, \quad (10)$$

$$\left(\frac{1}{Pr}\right)\theta'' + f\theta' + Nb\phi'\theta' + Nt\theta'^2 = 0, \quad (11)$$

$$\phi'' + Lef\phi' + Nt_b\theta'' = 0, \quad (12)$$

Where

$$\lambda = \frac{Gr_x}{Re_x}, \delta = \frac{Gc_x}{Re_x}, M = \frac{\sigma {B_0}^2(x)}{a\rho}, K_1 = \frac{\nu}{ak}, Le = \frac{\nu}{D_B} Pr = \frac{\nu}{\alpha}, N_b = \frac{\tau D_B(C_w-C_\infty)}{\nu}, N_t = \frac{\tau D_t(T_w-T_\infty)}{\nu T_\infty},$$

$$Nt_b = \frac{N_t}{N_b}, Gr_x = \frac{g\beta_t(T_w-T_\infty)x}{a\nu}, Re_x = \frac{u_w(x)x}{\nu}, Gc_x = \frac{g\beta_c(C_w-C_\infty)x}{a\nu} \quad (13)$$

Here, primes means the differentiation concerning η, λ Buoyancy constraint, Solutal buoyancy parameter is given by δ, the magnetic parameter is given by M, kinematic viscidness of the liquid is denoted by ν, Pr denotes the Prandtl number, Le denotes the Lewis number, K_1 represents permeability factor, K is the dimensionless vertex thickness.

The corresponding boundary conditions are transformed to

$$f(\eta) = 0, \quad f'(\eta) = 0, \ \theta(\eta) = 1, \ \phi(\eta) = 1 \quad at \ \eta = 0,$$

$$f'(\eta) \to 0, \quad \theta(\eta) \to 0, \ \phi(\eta) \to 0 \ as \ \eta \to \infty, \quad (14)$$

The skin friction, Sherwood number and Nusselt number for the present problem are defined as

$$Nu_x = \frac{xq_w}{k(T_w-T_\infty)}, Sh_x = \frac{xq_m}{D_B(C_w-C_\infty)}, C_f = \frac{t_w}{{u_w}^2\rho_f} \quad (15)$$

The related terms for the skin-friction factor $C_{fx}(0) = f''(0)$, the reduced Nusselt number $-\theta'(0)$ and the reduced Sherwood number $-\phi'(0)$ are defined as

$$-\theta'(0) = \frac{Nu_x}{\sqrt{Re_x}}, -\phi'(0) = \frac{Sh_x}{\sqrt{Re_x}}, C_{fx} = C_f\sqrt{Re_x} \quad (16)$$

Where, $Re_x = \frac{u_w(x)x}{\nu}$, is the local Reynolds number built on the extending velocity. The converted nonlinear differential equations (9) to (12) by applying equation (14) are elucidated by Keller box scheme consisting on the steps as, finite-differences technique, Newton's scheme and block elimination process clearly explained by Anwar et al. [35].

3 Results and Discussion

This portion of study deals with the calculated results of converted nonlinear ordinary differential equations (9-12) with boundary conditions (14) solved via Killer-box method. For numerical result of physical parameters of our concern including Brownian motion constraint Nb, thermophoresis constraint Nt, magnetic factor M, buoyancy factor λ, solutal buoyancy factor δ, inclination factor γ, Prandtl number Pr, Lewis number Le, and material factor K several figures and tables are prepared. In Table 3.1, in the deficiency of buoyancy factor λ, solutal buoyancy factor δ, magnetic factor M, porosity parameter K_1 and material parameter K with γ = 90^o outcomes for reduced Nusselt number $-\theta'(0)$, reduced Sherwood number $-\phi'(0)$ are equated with the existing results of Khan and Pop [36]. The consequences are established brilliant settlement. The effects of reduced Nusselt number $-\theta'(0)$, reduced Sherwood number $-\phi'(0)$ and skin friction coefficient $C_{fx}(0)$ against altered values of involved physical parameters $Nb, Nt, M, K, \lambda, \delta, \gamma, K_1, Le$, and Pr are shown in table 3.2. It is eminent that $-\theta'(0)$ declines for increasing the values of Nb,Nt, M,Le, K_1, γ, and increased by enhancing the numerical values of K, λ, δ, and Pr. Moreover, it is perceived that $-\phi'(0)$ enhanced with the larger values of $Nb, \lambda, \delta, Nt, Le$, $K$and drops for bigger values of $M, K_1,\ Pr$ and γ. On the other hand, $C_{fx}(0)$ rises with the growing values of Nb, Le, M, K, γ, K_1, and drops with the higher values of Nt, λ, δ, and Pr.

Table 3.1: Contrast of the reduced Nusselt number $-\theta'(0)$ and the reduced Sherwood number $-\phi'(0)$ when M, K, K1, δ, λ = 0, Pr = Le = 10 and γ= 90°.

Nb	***Nt***	Khan and Pop (2010)		Present Results	
		$-\theta'(0)$	$-\phi'(0)$	$-\theta'(0)$	$-\phi'(0)$
0.1	0.1	0.9524	2.1294	0.9524	2.1294
0.2	0.2	0.3654	2.5152	0.3654	2.5152
0.3	0.3	0.1355	2.6088	0.1355	2.6088
0.4	0.4	0.0495	2.6038	0.0495	2.6038
0.5	0.5	0.0179	2.5731	0.0179	2.5731

Table 3.2: Values of the reduced Nusselt number $-\theta'(0)$, the reduced Sherwood number $-\phi'(0)$ and the Skin-friction coefficient $C_{fx}(0)$.

Nb	***Nt***	**Pr**	***Le***	***M***	***K***	***λ***	***δ***	***K1***	***γ***	$-\theta'(0)$	$-\phi'(0)$	$C_{fx}(0)$
0.1	0.1	7.0	5.0	0.5	1.0	0.1	0.9	1.0	45^0	1.1054	1.0880	1.8913
0.5	0.1	7.0	5.0	0.5	1.0	0.1	0.9	1.0	45^0	0.2060	1.6011	1.9459
0.1	**0.5**	7.0	5.0	0.5	1.0	0.1	0.9	1.0	45^0	0.5104	1.3906	1.7176
0.1	0.1	**10.0**	5.0	0.5	1.0	0.1	0.9	1.0	45^0	1.1531	1.0852	1.8882
0.1	0.1	7.0	**10.0**	0.5	1.0	0.1	0.9	1.0	45^0	0.9672	2.0567	1.9689
0.1	0.1	7.0	5.0	**1.0**	1.0	0.1	0.9	1.0	45^0	1.0949	1.0550	2.1075
0.1	0.1	7.0	5.0	0.5	**3.0**	0.1	0.9	1.0	45^0	1.1331	1.1755	2.6215
0.1	0.1	7.0	5.0	0.5	1.0	**0.5**	0.9	1.0	45^0	1.1090	1.0963	1.8040
0.1	0.1	7.0	5.0	0.5	1.0	0.1	**2.0**	1.0	45^0	1.1195	1.1254	1.5847
0.1	0.1	7.0	5.0	0.5	1.0	0.1	0.9	**2.0**	45^0	1.0851	1.0246	2.3071
0.1	0.1	7.0	5.0	0.5	1.0	0.1	0.9	1.0	$\mathbf{90^0}$	1.0917	1.0507	2.1758

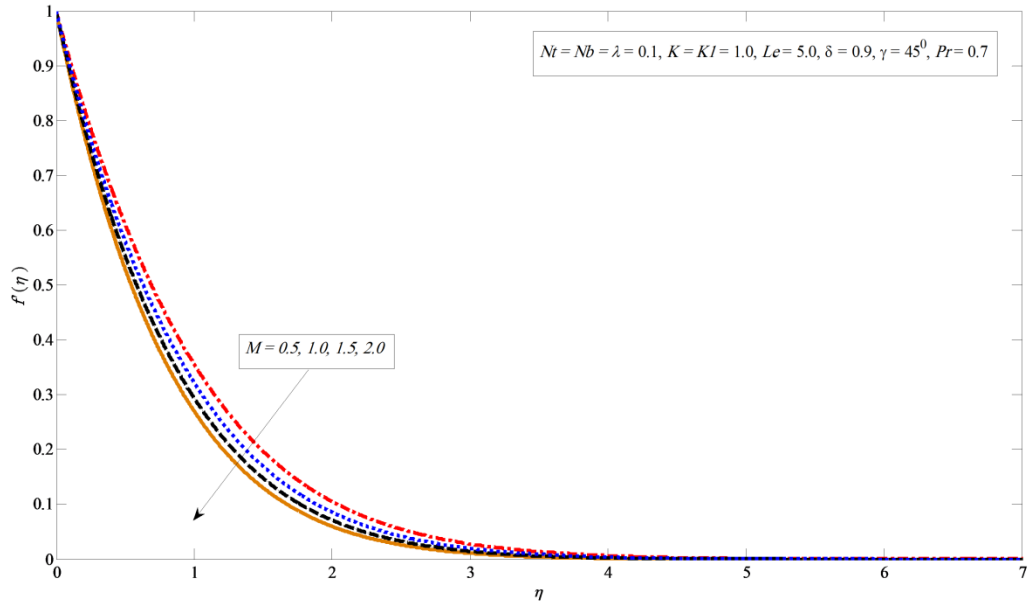

Fig. 2. Variations in velocity profile for several values of M.

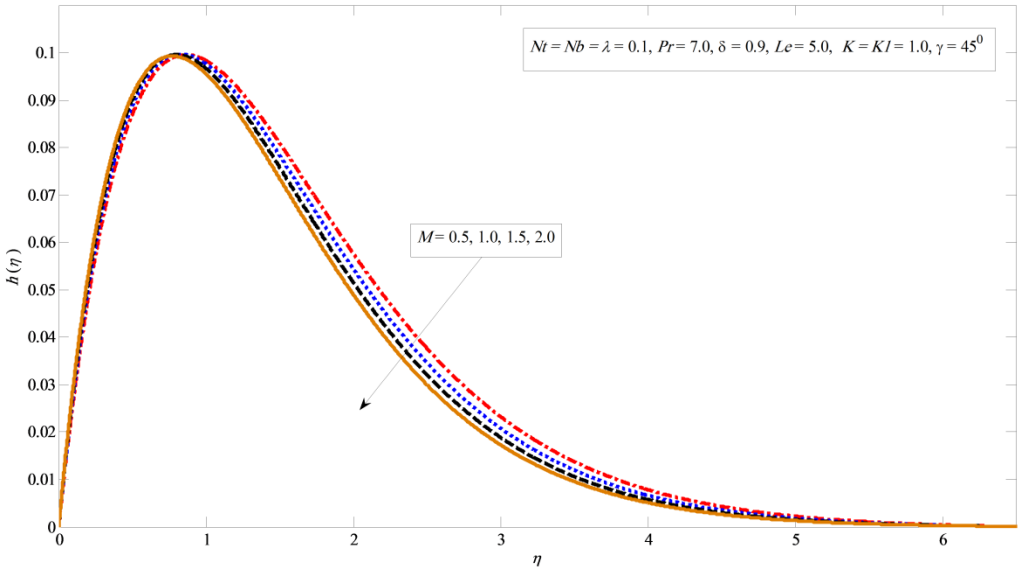

Fig. 3. Variations in angular velocity for several values of M.

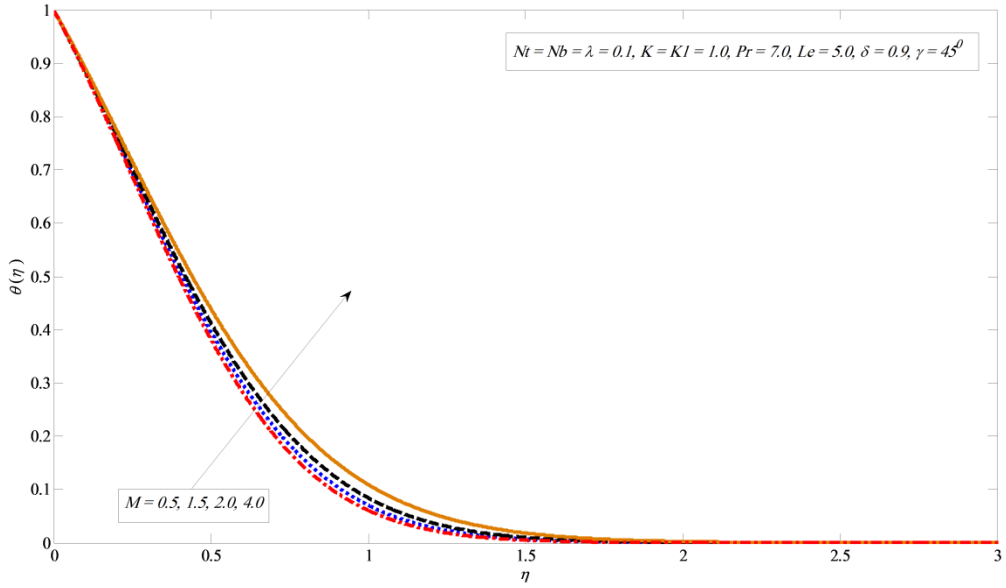

Fig. 4. Variations in temperature profile for several values of M.

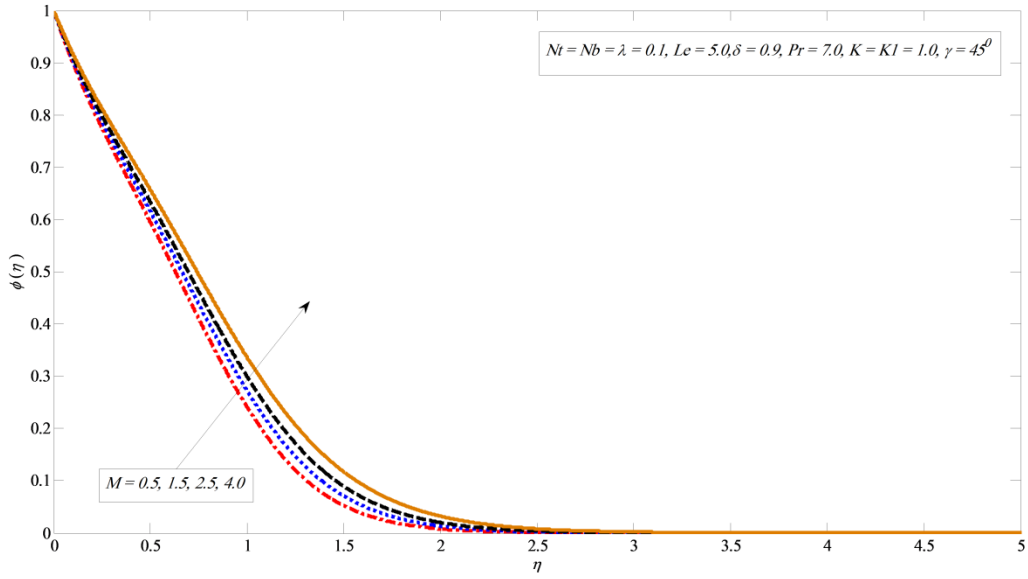

Fig. 5. Variations in concentration profile for several values of M.

Fig. 2 gives a picture of the upshot of factor M on velocity profile. The velocity outline slows down as we upsurge the magnetic field constraint M. It is seen the use of magnetic field yields Lorentz force, by means retard the speed of the fluid. The similar result has seen in the instance of the angular velocity against changed values of M in Fig. 3. Whereas, the different impacts of M on the temperature distribution are presented in Fig. 4 and concentration profile in Fig. 5.

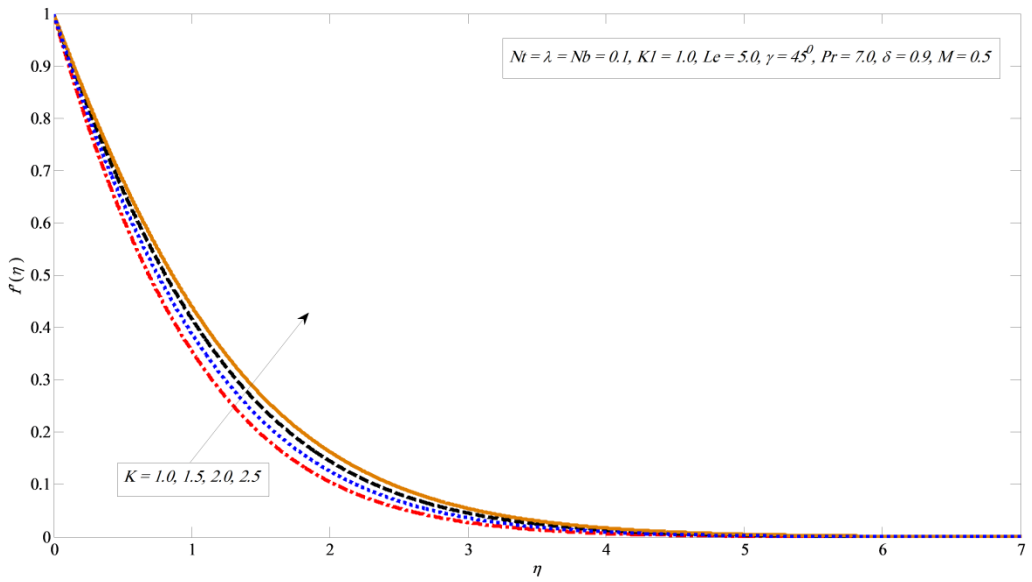

231

232 Fig. 6. Variations in velocity profile for several values of K.

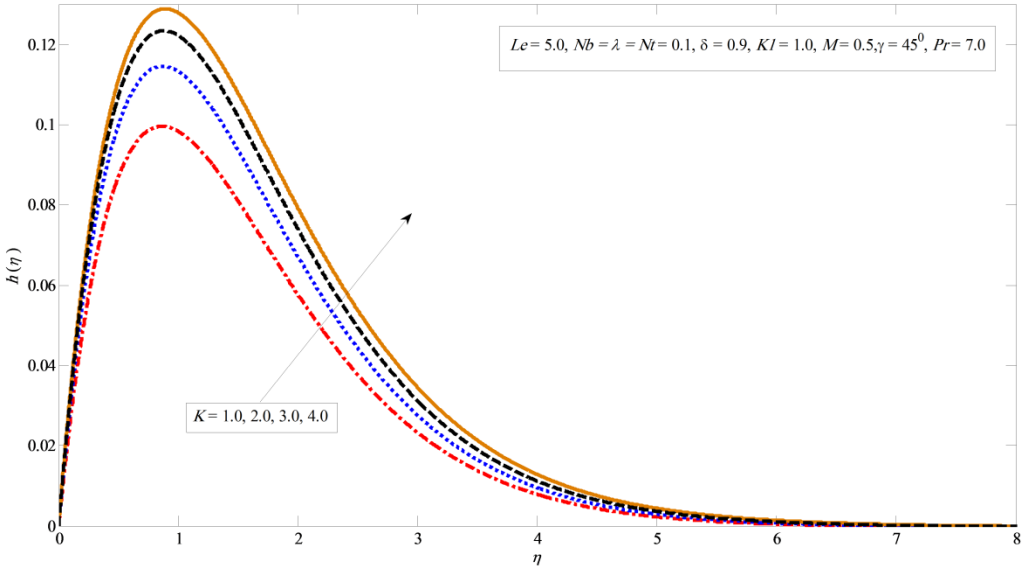

233

234 Fig. 7. Variations in angular velocity profile for several values of K.

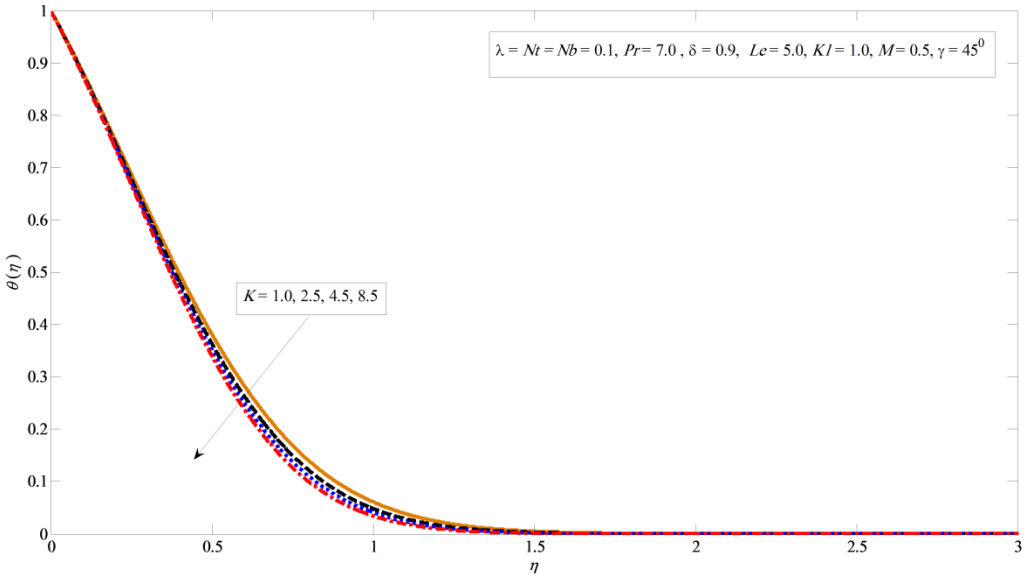

Fig. 8. Variations in temperature profile for several values of K.

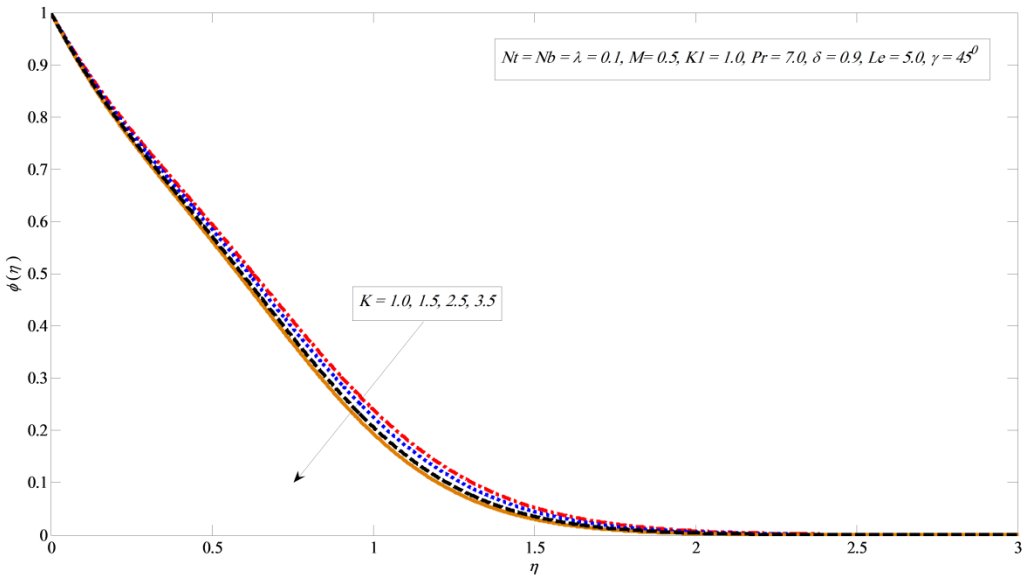

Fig. 9. Variations in concentration profile for several values of K.

It is noticed in Fig.6 the velocity profile upturn by enhancing the values of K. The angular velocity profile rise by growing the values of K is indicated in Fig. 7. The boundary layer thickness losses by improving the values of K. On the other hand, Figs. 8 and 9 depict the opposite effects against different values of K.

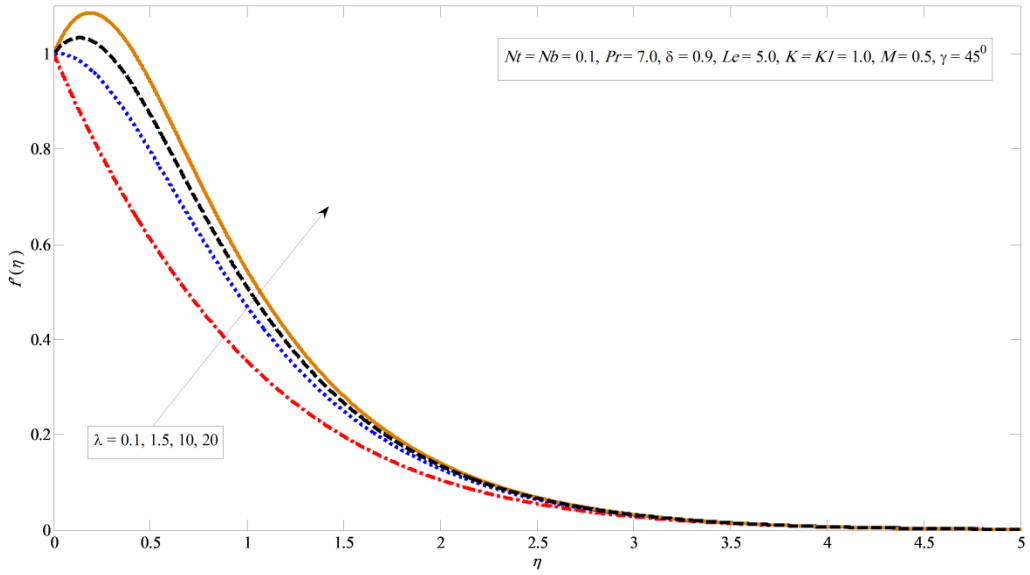

243

244 Fig. 10. Variations in velocity profile for several values of λ.

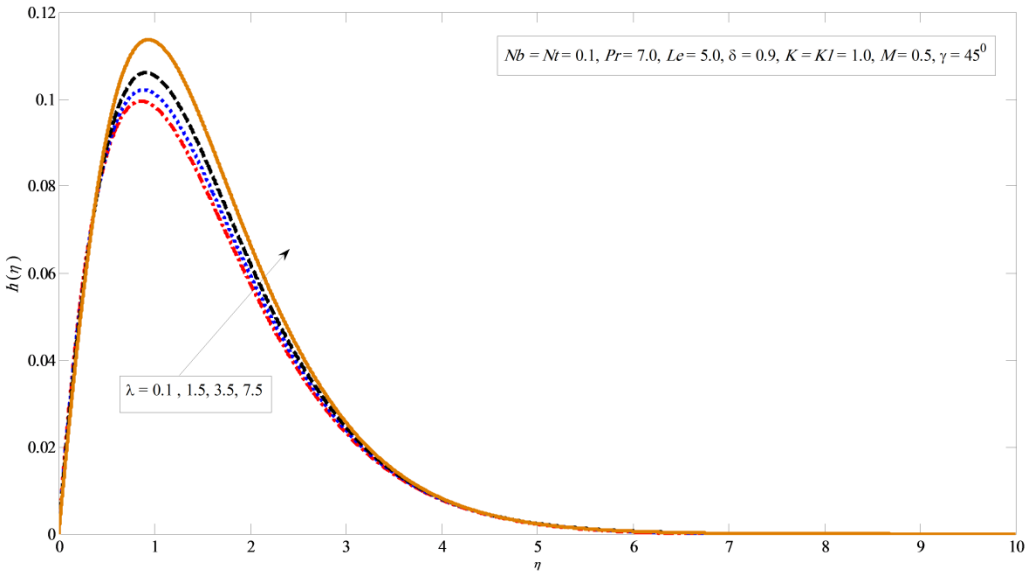

245

246 Fig. 11. Variation in angular velocity profile for several values of λ.

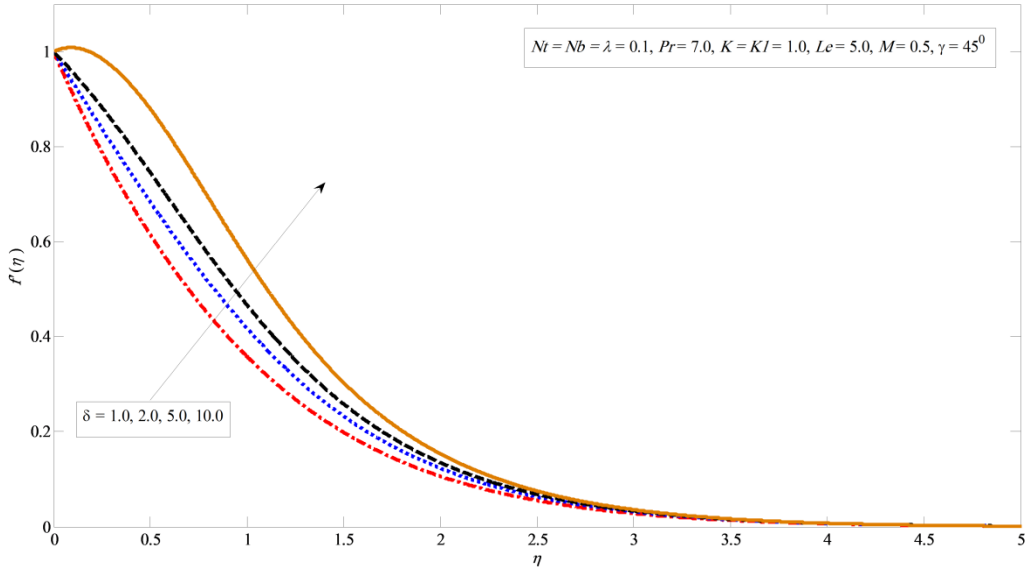

247

248 Fig. 12. Variations in velocity profile for several values of δ.

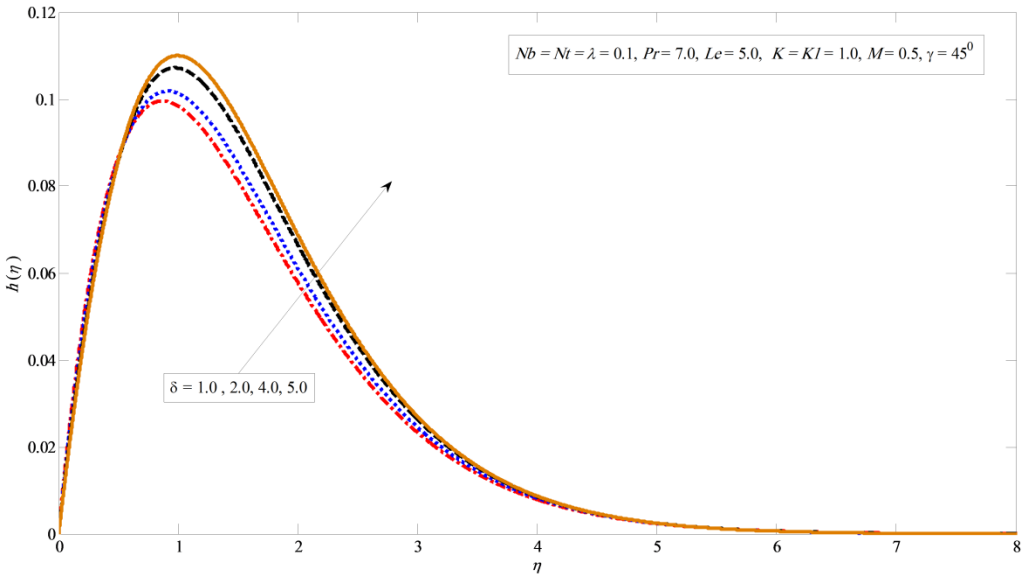

249

250 Fig. 13. Variations in angular velocity profile for several values of δ.

251 The velocity shape upturns in Fig. 10 by enhancing bouncy parameter λ. Similarly the angular
252 velocity also enhanced with large values of λ clearly shown in Fig. 11. Moreover, the similar
253 result for solutal bouncy parameter δ on velocity distribution and angular velocity contour is
254 prominent in Figs.12 and 13.

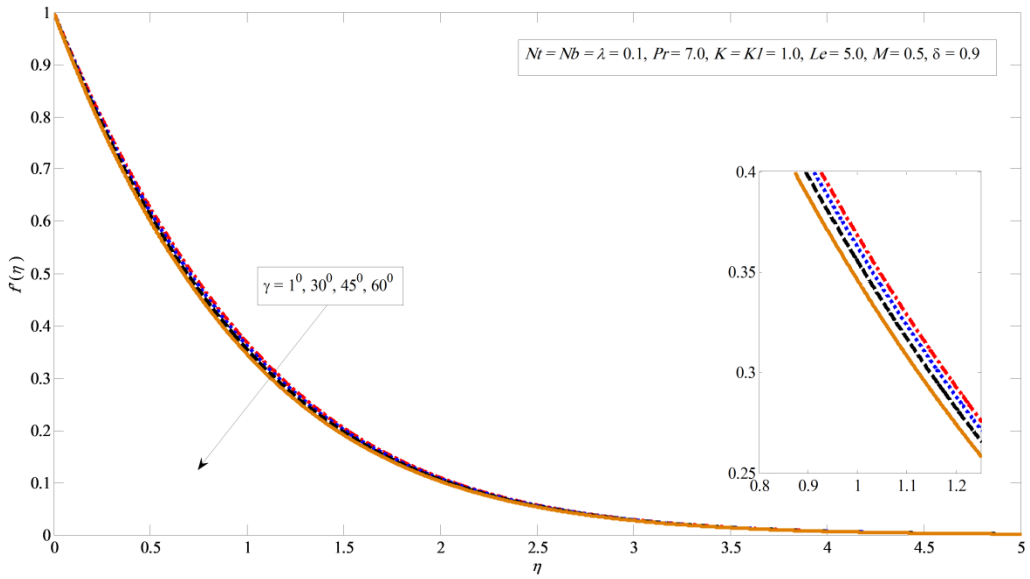

255

256 Fig. 14. Variations in velocity profile for several value of γ.

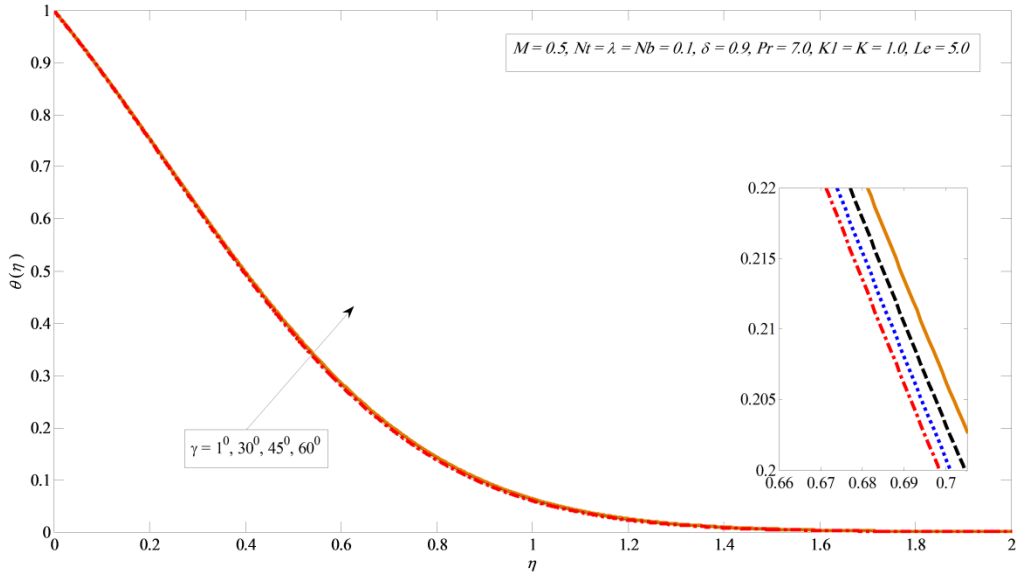

257

258 Fig. 15. Variations in temperature profile for several values of γ.

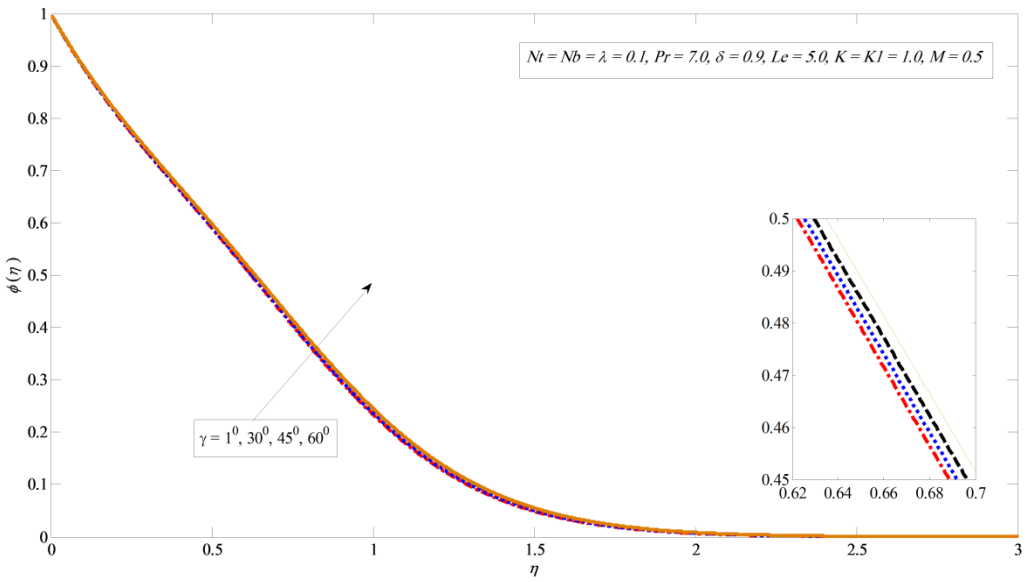

Fig. 16. Variations in concentration profile for several values of γ.

Fig. 14 portrays the consequence of inclination factor γ on velocity outline. It is openly perceived the velocity outline depreciate as we enhance the values of inclination parameter γ. This can be ascribed to the circumstance that the maximum gravitational force act on flow when the inclination parameter $\gamma = 0$ because in this situation the sheet will be vertical. On the other hand, for $\gamma = 90^0$ the sheet will be horizontal which cause the reduction in the velocity profile as the strength of the bouncy forces decrease. Besides, opposite result are recovered in Figs. 15 and 16 for large values of inclination parameter γ in the instance of temperature and concentration sketches.

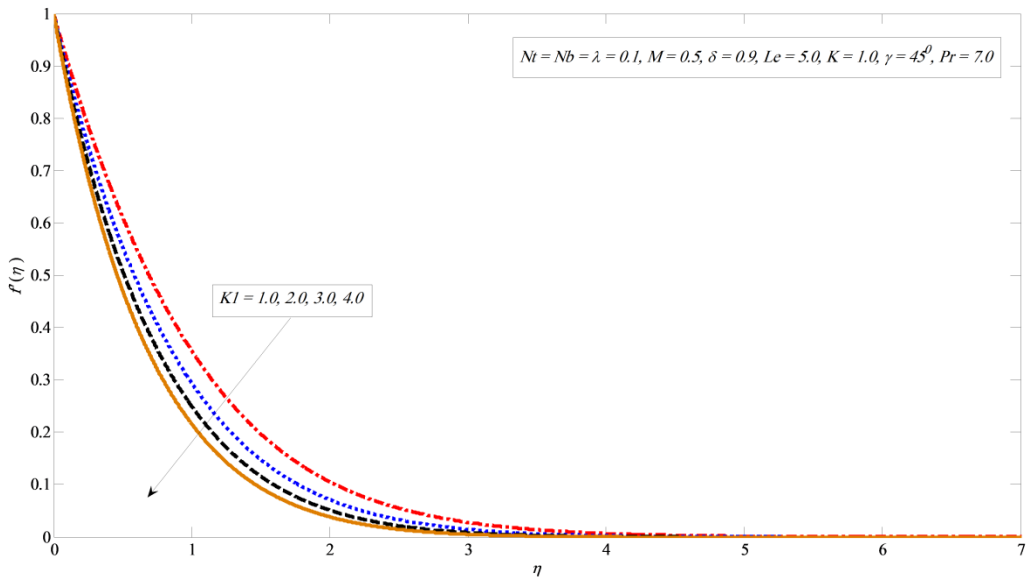

Fig. 17. Variations in velocity profile for several values of K_1.

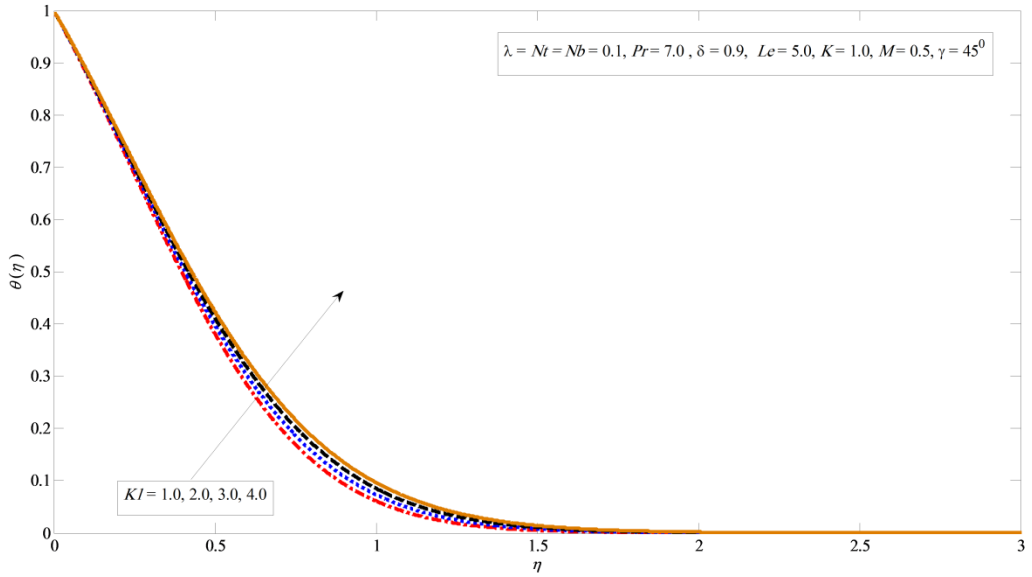

Fig. 18. Variations in temperature profile for several value of K_1.

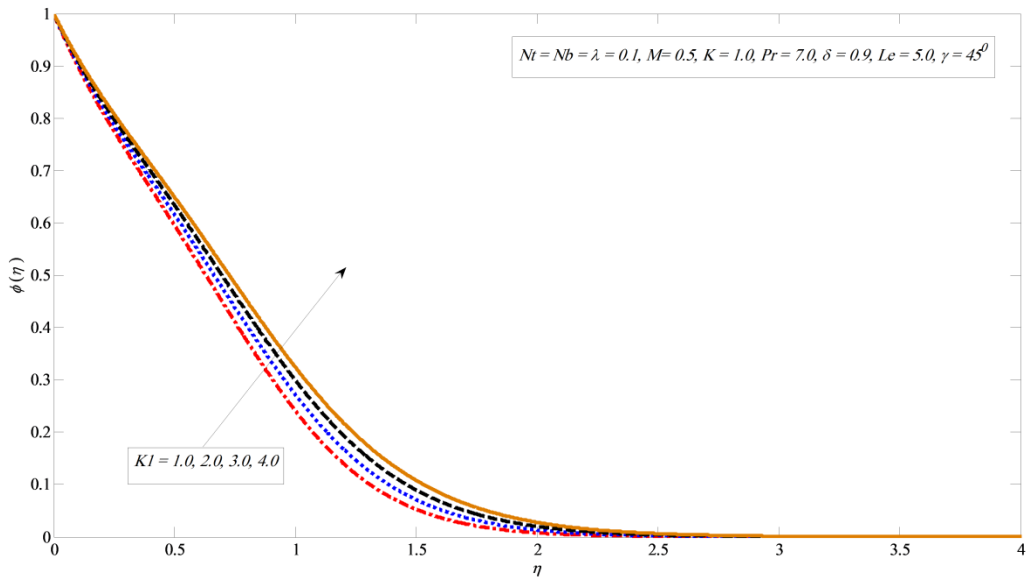

Fig. 19. Variations in concentration profile for several values of K_1.

It is well known that the porous medium offers high resistance that cause rising of shear stress. This shear stress work opposite to the fluid motion over a stretching sheet and fluid motion tends to slow. That's why, velocity profile illustrate reduction by increasing the values of K_1 in this case as indicated by Fig. 17. Moreover, oppoite impact is ilustrated in Figs. 18 and 19 for various values of K_1.

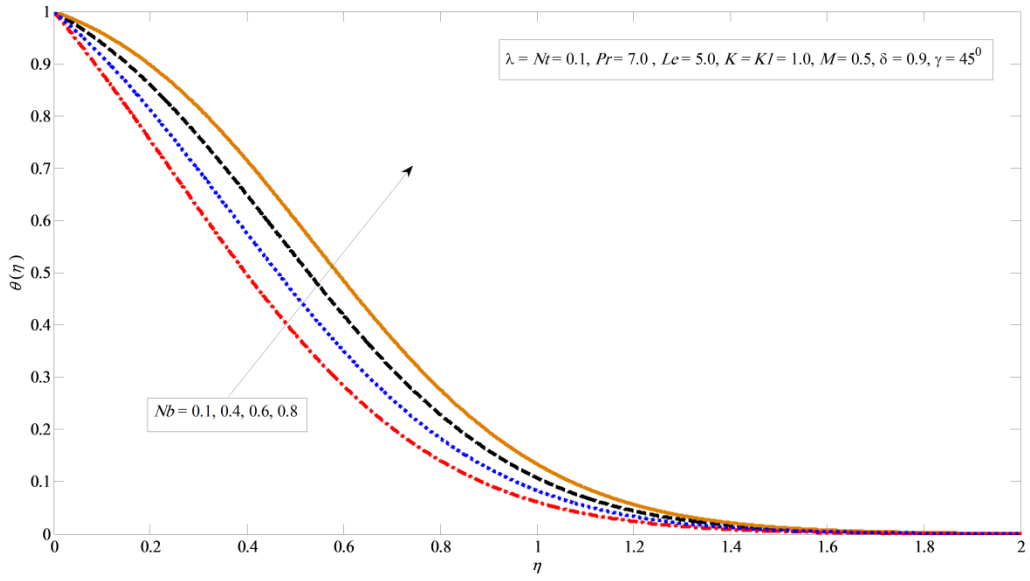

Fig. 20. Variations in temperature profile for several values of Nb.

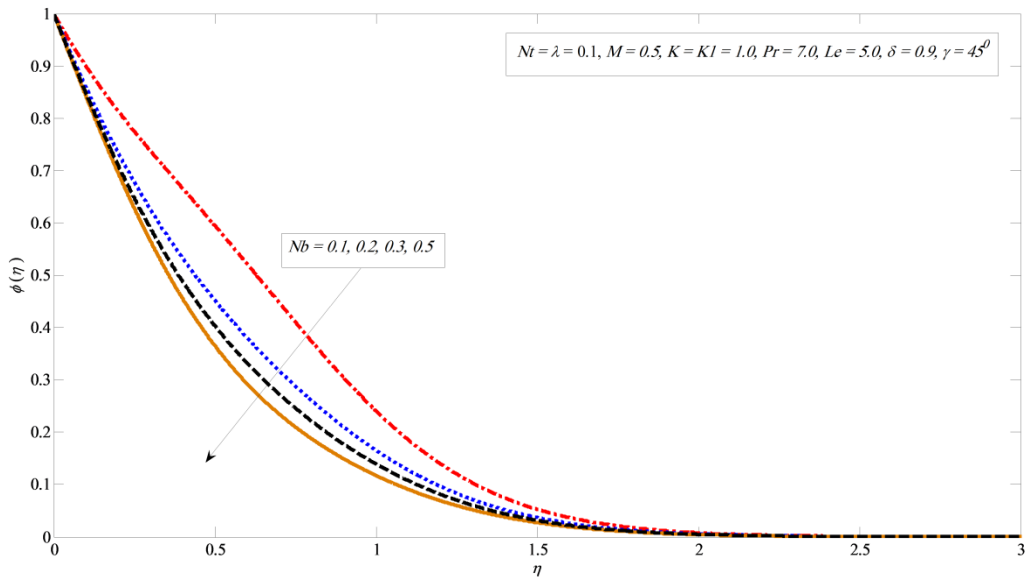

Fig. 21. Variations in concentration profile for several values of Nb.

Figures. 20 and 21 display the of effect of Brownian movement on the temperature and concentration sketches separately. The temperature sketch enlarges on enlarging Nb, on the other hand, concentration distribution enlighten dissimilar style. Physically, boundary layer heat up due to the development in Brownian motion which inclines to travel nanoparticles from the extending sheet to the motionless liquid. Therefore the absorption nanoparticle lessens.

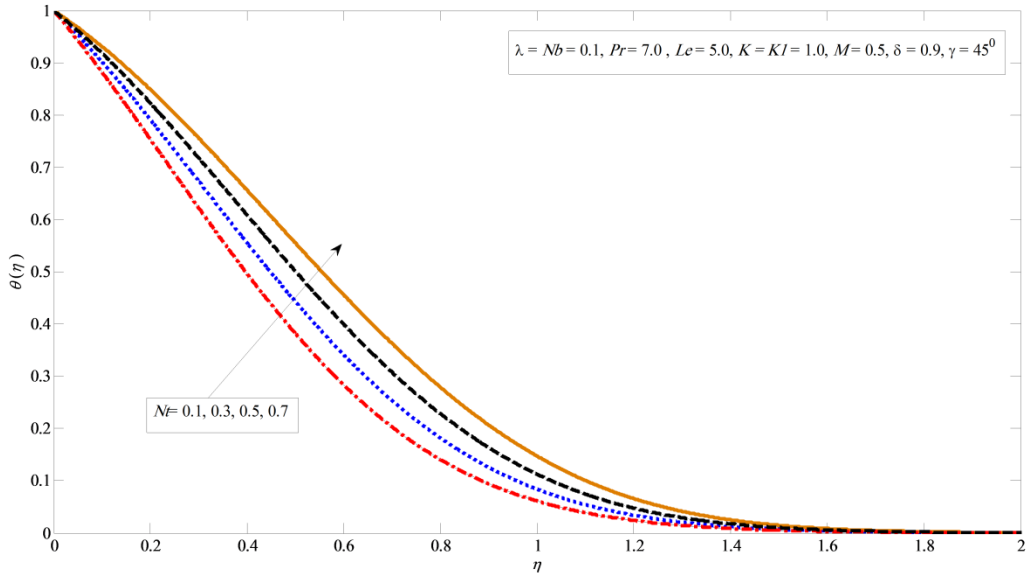

Fig. 22. Variations in temperature profile for several values of Nt.

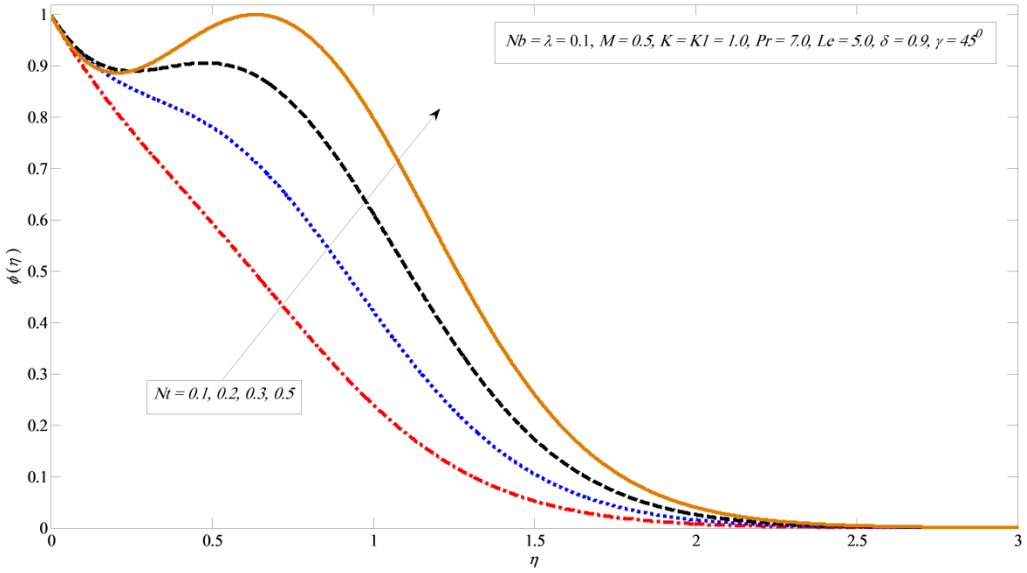

291

292 Fig. 23. Variations in concentration profile for several values of Nt.

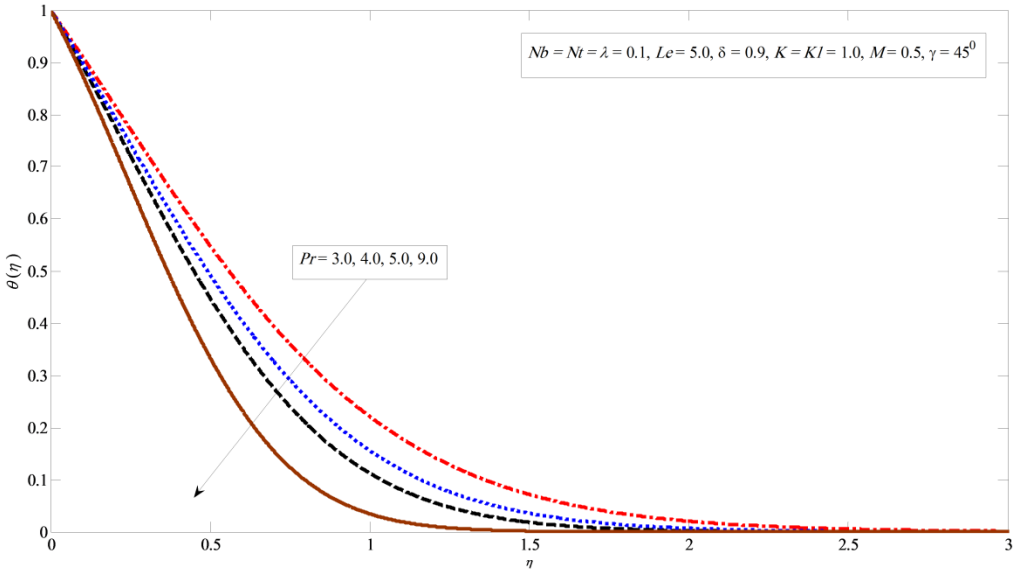

293

294 Fig. 24. Variations in temperature profile for several values of Pr.

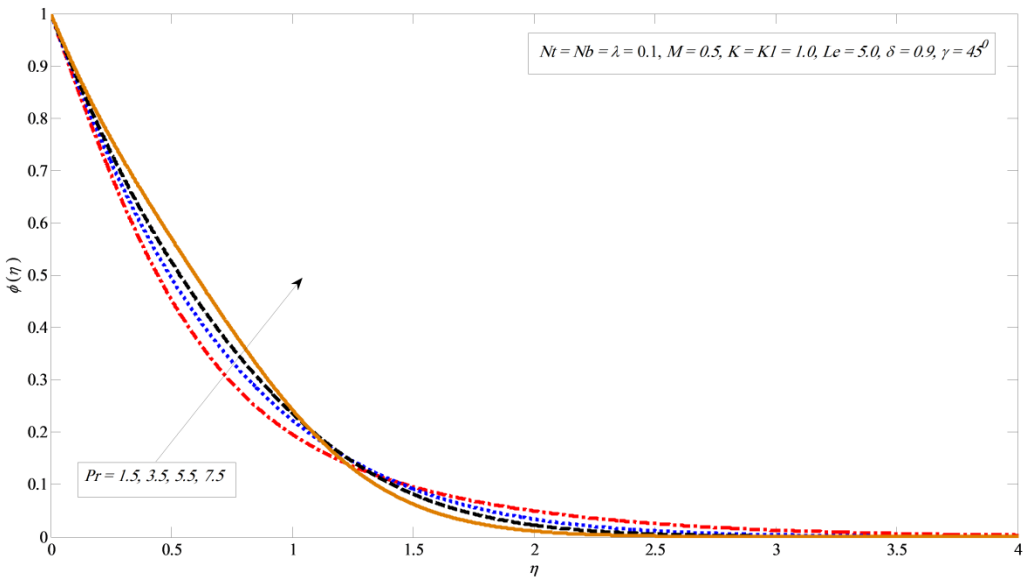

Fig. 25. Variations in concentration profile for several values of Pr.

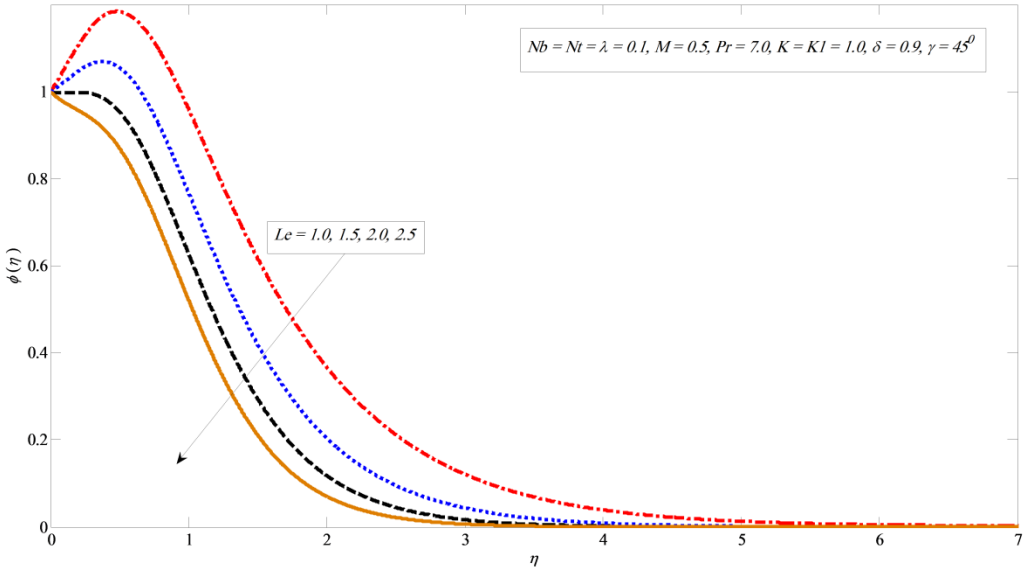

Fig. 26. Variations in concentration profile for several value of Le.

Figs. 22 and 23 present temperature and concentration profile against several values of thermophoresis parameters Nt. It is observed that both temperature and concentration contours upsurge by growing the thermophoresis parameter. Thermophoresis works to heat up boundary layer against several values of Prandtl number and Lewis number. Besides the amount of heat and mass exchange reduce by improving thermophoresis constraint Nt. Fig. 24 reveals that by

growing the values of Prandtl number factor Pr the temperature profile drop, because thermal boundary layer viscosity declining by growing the Prandtl number Pr. In short, an upturn in Prandtl number Pr mean deliberate amount of thermal dispersion. Whereas, concentration profile fall with large values of Pr presented in Fig. 25. Fig. 26 displays the result of Lewis number Le on concentration profile. The boundary layer viscosity lessening by improving the values of Lewis number Le.

4 Conclusions

This study has explored the heat and mass exchange of micropolar nanofluid flow over linear inclined extending sheet. It is noted that $-\theta'(0)$ falls for growing the values of Nb,Nt, M,Le, K_1, γ, and improved by enhancing the numerical values of K, λ, δ, and Pr. Moreover, it is observed that $-\phi'(0)$ boosted with the larger values of Nb, λ, δ, Nt, Le, $K$and falls for bigger values of M, K_1, Pr and γ. On the other hand, $C_{fx}(0)$ rises with the cumulative values of Nb, Le, M, K, γ, K_1, and falls with the higher values of Nt, λ, δ, and Pr.

Ethical: NA

Consent: NA

References

[1**]** Choi, S. U. S., Singer, D. A., & Wang, H. P. (1995). Developments and applications of non-Newtonian flows. *ASME FED*, *66*, 99–105.

[2] Buongiorno, J. (2006). Convective transport in nanofluids. *Journal of Heat Transfer*, *128*(3), 240–250.

[3**]** Zaimi, K., Ishak, A., & Pop, I. (2014). Boundary layer flow and heat transfer over a nonlinearly permeable stretching/shrinking sheet in a nanofluid. *Scientific Reports*, *4*, 4404.

[4] Anwar, M. I., Khan, I., Sharidan, S., & Salleh, M. Z. (2012). Conjugate effects of heat and mass transfer of nanofluids over a nonlinear stretching sheet. *International Journal of Physical Sciences*, *7*(26), 4081-4092.

[5] Sandeep, N., & Kumar, M. S. (2016). Heat and Mass Transfer in Nanofluid Flow over an Inclined Stretching Sheet with Volume Fraction of Dust and Nanoparticles. *Journal of Applied Fluid Mechanics*, *9*(5).

[6] Suriyakumar, P., & Devi, S. A. (2015). Effects of Suction and Internal Heat Generation on Hydromagnetic Mixed Convective Nanofluid Flow over an Inclined Stretching

Plate. *European journal of advances in engineering and technology*, *2*(3), 51-58.

[7] Ziaei-Rad, M., Kasaeipoor, A., Rashidi, M. M., & Lorenzini, G. (2017). A Similarity Solution for Mixed-Convection Boundary Layer Nanofluid Flow on an Inclined Permeable Surface. *Journal of Thermal Science and Engineering Applications*, (c). https://doi.org/10.1115/1.4035733

[8] Rashad, A. (2017). Unsteady nanofluid flow over an inclined stretching surface with convective boundary condition and anisotropic slip impact. *International Journal of Heat and Technology*, *35*(1), 82–90. https://doi.org/10.18280/ijht.350111

[9] Mitra, A. (2018). Computational Modelling of Boundary-Layer Flow of a Nano fluid Over a Convective Heated Inclined Plate. *JOURNAL OF MECHANICS OF CONTINUA AND MATHEMATICAL SCIENCES*, *13*(2), 88-94.

[10] Khan, M., Shahid, A., Malik, M. Y., & Salahuddin, T. (2018). Thermal and concentration diffusion in Jeffery nanofluid flow over an inclined stretching sheet: A generalized Fourier's and Fick's perspective. *Journal of Molecular Liquids*, *251*, 7–14.

[11] Hatami, M., Jing, D., & Yousif, M. A. (2018). Three-dimensional analysis of condensation nanofluid film on an inclined rotating disk by efficient analytical methods. *Arab Journal of Basic and Applied Sciences*, *25*(1), 28–37.

[12] Mjankwi, M. A., Masanja, V. G., Mureithi, E. W., & James, M. N. O. (2019). Unsteady MHD Flow of Nanofluid with Variable Properties over a Stretching Sheet in the Presence of Thermal Radiation and Chemical Reaction. *International Journal of Mathematics and Mathematical Sciences*, *2019*.

[13] Saeed, A., Shah, Z., Islam, S., Jawad, M., Ullah, A., Gul, T., & Kumam, P. (2019). Three-Dimensional Casson Nanofluid Thin Film Flow over an Inclined Rotating Disk with the Impact of Heat Generation/Consumption and Thermal Radiation. *Coatings*, *9*(4), 248.

[14] Rafique, K., Anwar, M. I., & Misiran, M. (2019). Keller-box Study on Casson Nano Fluid Flow over a Slanted Permeable Surface with Chemical Reaction. *Asian Research Journal of Mathematics*, 1-17.

[15] Sakiadis, B. C. (1961). Boundary-layer behavior on continuous solid surfaces: I. Boundary-layer equations for two-dimensional and axisymmetric flow. *AIChE Journal*, *7*(1), 26–28.

[16] Crane, L. J. (1970). Flow past a stretching plate. *Zeitschrift Für Angewandte Mathematik Und Physik (ZAMP)*, *21*(4), 645–647.

[17] Ramesh, G. K., Gireesha, B. J., & Bagewadi, C. S. (2012). Heat transfer in MHD dusty boundary layer flow over an inclined stretching sheet with non-uniform heat source/sink. *Advances in Mathematical Physics*, *2012*.

[18] Singh, P. K. (2012). Heat and mass transfer in MHD boundary layer flow past an inclined plate with viscous dissipation in porous medium. *International Journal of Scientific &*

374 *Engineering Research*, *3*(6), 1–11.

375 [19] Ali, M., Alim, M. A., & Alam, M. S. (2015). Similarity Solution of Heat and Mass Transfer
376 Flow over an Inclined Stretching Sheet with Viscous Dissipation and Constant Heat Flux in
377 Presence of Magnetic Field. *Procedia Engineering*, *105*(Icte 2014), 557–569.
378 https://doi.org/10.1016/j.proeng.2015.05.089

379 [20] Ramesh, G. K., Chamkha, A. J., & Gireesha, B. J. (2015). Boundary layer flow past an
380 inclined stationary/moving flat plate with convective boundary condition. *Afrika*
381 *Matematika*. https://doi.org/10.1007/s13370-015-0323-x

382 [21] Malik, M. Y., & Rehman, K. U. (2016). Effects of second order chemical reaction on MHD
383 free convection dissipative fluid flow past an inclined porous surface by way of heat
384 generation: A Lie group analysis. *Information Sciences Letters*, *5*, 35-45.

385 [22] Hayat, T., Qayyum, S., Alsaedi, A., & Asghar, S. (2017). Radiation effects on the mixed
386 convection flow induced by an inclined stretching cylinder with non-uniform heat
387 source/sink. *PloS one*, *12*(4), e0175584.

388 [23] Balla, C. S., Kishan, N., Gorla, R. S. R., & Gireesha, B. J. (2017). MHD boundary layer
389 flow and heat transfer in an inclined porous square cavity filled with nanofluids. *Ain Shams*
390 *Engineering Journal*, *8*(2), 237–254.

391 [24] Tlili, I. (2019). Effects MHD and Heat Generation on Mixed Convection Flow of Jeffrey
392 Fluid in Microgravity Environment over an Inclined Stretching Sheet. *Symmetry*, *11*(3),
393 438.

394 [25] Jain, S., & Parmar, A. (2018). Multiple slip effects on inclined MHD Casson fluid flow over
395 a permeable stretching surface and a melting surface. *INTERNATIONAL JOURNAL OF*
396 *HEAT AND TECHNOLOGY*, *36*(2), 585-594.

397

398 [26] Eringen, A. C. (1964). Simple microfluids. *International Journal of Engineering Science*,
399 *2*(2), 205–217.

400 [27] Rahman, M. M., Aziz, A., & Al-Lawatia, M. A. (2010). Heat transfer in micropolar fluid
401 along an inclined permeable plate with variable fluid properties. *International Journal of*
402 *Thermal Sciences*, *49*(6), 993–1002. https://doi.org/10.1016/j.ijthermalsci.2010.01.002

403 [28] Das, K. (2012). Slip effects on heat and mass transfer in MHD micropolar fluid flow over an
404 inclined plate with thermal radiation and chemical reaction. *International Journal for*
405 *Numerical Methods in Fluids*, *70*(1), 96–113.

406 [29] Kasim, A. R. M., Mohammad, N. F., & Shafie, S. (2013). Unsteady MHD mixed convection
407 flow of a micropolar fluid along an inclined stretching plate. *Heat Transfer—Asian*
408 *Research*, *42*(2), 89–99.

409 [30] Srinivasacharya, D., & Bindu, K. H. (2016). Entropy generation in a micropolar fluid flow
410 through an inclined channel. *Alexandria Engineering Journal*, *55*(2), 973–982.

[31] Hazbavi, A., & Sharhani, S. (2017). Micropolar Fluid Flow Between Two Inclined Parallel Plates. In *ASME 2017 International Mechanical Engineering Congress and Exposition* (p. V008T10A085-V008T10A085). American Society of Mechanical Engineers.

[32] Shamshuddin, M. D., Mishra, S. R., Bég, O. A., & Kadir, A. (2018). Unsteady reactive magnetic radiative micropolar flow, heat and mass transfer from an inclined plate with joule heating: A model for magnetic polymer processing. *Proceedings of the Institution of Mechanical Engineers, Part C: Journal of Mechanical Engineering Science*, 954406218768837.

[33] Srinivasacharya, D., RamReddy, C., & Naveen, P. (2018). Double dispersion effect on nonlinear convective flow over an inclined plate in a micropolar fluid saturated non-Darcy porous medium. *Engineering Science and Technology, an International Journal*.

[34] Mishra, S. R., Baag, S., & Mohapatra, D. K. (2016). Engineering Science and Technology , an International Journal Chemical reaction and Soret effects on hydromagnetic micropolar fluid along a stretching sheet. *Engineering Science and Technology, an International Journal*, *19*(4), 1919–1928. https://doi.org/10.1016/j.jestch.2016.07.016

[35] Anwar, M. I., Shafie, S., Hayat, T., Shehzad, S. A., & Salleh, M. Z. (2017b). Numerical study for MHD stagnation-point flow of a micropolar nanofluid towards a stretching sheet. *Journal of the Brazilian Society of Mechanical Sciences and Engineering*, *39*(1), 89–100. https://doi.org/10.1007/s40430-016-0610-y

[36] Khan, W. A., & Pop, I. (2010). Boundary-layer flow of a nanofluid past a stretching sheet. *International journal of heat and mass transfer*, *53*(11-12), 2477-2483.

[37] Rafique, K., Anwar, M. I., & Misiran, M. (2019). Keller-box Study on Casson Nano Fluid Flow over a Slanted Permeable Surface with Chemical Reaction. *Asian Research Journal of Mathematics*, 1-17.